



ELSEVIER

Polymer 44 (2003) 377–387

polymerwww.elsevier.com/locate/polymer

Analysis of the solvent diffusion in glassy polymer films using a set inversion method

Anne-Claire Dubreuil^a, Frédéric Doumenc^a, Béatrice Guerrier^{a,*}, Diethelm Johannsmann^b, Catherine Allain^a

^aLab. FAST, Université Pierre et Marie Curie—Université Paris Sud—CNRS, Bât. 502, Campus Universitaire, 91405 Orsay, France

^bMax Planck Institute for Polymer Research, Ackermannweg 10, 55128 Mainz, Germany

Received 15 May 2002; received in revised form 10 September 2002; accepted 10 October 2002

Abstract

Within the framework of solvent diffusion in glassy polymers, this paper concerns an experimental study of toluene sorption and desorption in P(MMA/*n*BMA) copolymer films. Gravimetric experiments (quartz microbalance) are performed in a pressure and temperature controlled chamber. Coupling between solvent diffusion and viscoelastic relaxation is taken into account through the time-dependent solubility model, based on the Fick diffusion equation inside the film and a time variable boundary condition at the film/vapor interface. Viscoelastic relaxation is described by a first order model or by a stretched exponential. In the present paper, a special focus is given on the set inversion method used to analyze the data and to derive well-defined uncertainty intervals upon each determined quantity, taking all the uncertainties on the weight measurements into account. We find that the mutual diffusion coefficient strongly decreases in the glassy state, of about two orders of magnitude for a 0.05 decrease in the solvent weight fraction.

© 2002 Elsevier Science Ltd. All rights reserved.

Keywords: Glass transition; Polymer/solvent mutual diffusion; Set inversion method

1. Introduction

Diffusion of solvents or low molecular weight species in polymer films or membranes is the determining factor in many processes such as the drying of polymer coatings, drug release, etc. From a fundamental point of view there is a large interest in the diffusion in in-homogeneous or complex systems which involve diffusion coefficients exhibiting large variations. Moreover, complex phenomena occur when diffusion is coupled to the glass transition and recent studies are dedicated to the glass transition and aging in glassy materials.

Within the framework of solvent diffusion in glassy polymers, this paper is devoted to an experimental study of solvent sorption and desorption in P(MMA/*n*BMA) copolymer films. Toluene is the solvent. In the glassy domain the coupling between diffusion and viscoelastic relaxation leads to complex kinetics for the film weight. Indeed, the relaxation of the stresses induced by volume variations

involves slow rearrangements of macromolecular chains. When the time scales characterizing diffusion and relaxation are comparable, it is well known that the kinetic is no more Fickian. Although numerous works have been devoted to this problem (see references in Section 4) the involved phenomena are not yet completely understood. Experimental investigations about the evolution of the mutual diffusion coefficient in the glassy domain have been performed for a few systems only and they show rather contradictory conclusions about the influence of glass transition. In order to study the non-Fickian sorption and desorption kinetics and the variations with the concentration of the polymer/solvent mutual diffusion coefficient D_{SP} , differential increasing and decreasing pressure steps were performed. We used a gravimetric technique based on a quartz crystal microbalance placed in a controlled solvent vapor pressure chamber.

Moreover, the coupling of diffusion and viscoelastic relaxation complicates the quantitative interpretation of experiments. A special focus is given in this paper on the method used to analyze the data and to reliably derived diffusion coefficients. We use the time-dependent solubility model, based on the Fick diffusion equation inside the film

* Corresponding author. Tel.: +33-1-69-15-80-63; fax: +33-1-69-15-80-60.

E-mail address: guerrier@fast.u-psud.fr (B. Guerrier).

and a boundary condition varying with time at the film/vapor interface. This model describes the coupled diffusion and relaxation phenomena with only four parameters, which are the characteristic times of relaxation and diffusion, the final value of the solvent content and the relative importance of diffusion- and relaxation-induced weight variations. To get a reliable estimate of these parameters we have used a set inversion method that aims to characterize all the parameters sets which are compatible with the experimental data, i.e. for which the model responses hold between two limiting curves surrounding the experimental one. These limiting curves enable to take all the uncertainties on the weight measurements into account and provide well-defined uncertainty intervals for each fit parameter. With such a method it is also possible to study the influence of the relaxation description on the estimated diffusion and relaxation parameters. Two solubility models were compared. In the first one, the relaxation is described by only one characteristic time. This simple description is clearly an approximation, since most experiments on the dynamics in glassy systems have been more successfully fitted with a stretched exponential corresponding to a broad distribution of relaxation times. The whole estimation procedure was then repeated with this description and the robustness of the results was analyzed.

The paper is organized as follows: synthesis and characterization of the polymers as well as sample preparation are described in Section 2. The experimental setup and procedure are described in Section 3. The time-dependent solubility model and relaxation descriptions are presented in Section 4. Section 5 is devoted to the set inversion method used to analyze the data. Qualitative and quantitative analysis of the experimental kinetics are detailed in Section 6 and compared to other experimental works.

2. Materials and sample preparation

2.1. Materials

The polymer samples used in this study were kindly prepared by Wagner and Stoehr (Max Planck Institute for Polymer Research, Mainz, Germany). Statistical methyl methacrylate/*n*-butyl methacrylate P(MMA/*n*BMA) copolymers were prepared by radical polymerization (see Ref. [1] for further details on synthesis and tacticities). Copolymer compositions were determined by comparing the intensities of the $-\text{OCH}_2-$ and $-\text{OCH}_3$ proton resonances, on the ^1H NMR spectra [2] (obtained in CDCl_3 on a 300 MHz AC-300 NMR spectrometer). The monomer proportions MMA/*n*BMA are 84/16 and 48/52. Molecular weights and polydispersities were determined by gel permeation chromatography, relative to PMMA standard, using a Waters

Table 1

Molecular weights M_n , polydispersities M_w/M_n and glass transition temperatures T_{g0} for the two P(MMA/*n*BMA) copolymers

Copolymer	M_n (kg/mol)	M_w/M_n	T_{g0} (°C)
84/16	91	2.93	96
48/52	207	2.34	63

apparatus. The glass transition temperatures T_{g0} ('mid-point' temperatures) were investigated by means of a Mettler DSC-30 differential scanning calorimeter. The heating rate was 10 °C/min. Molecular characteristics and calorimetric data are summarized in Table 1. Toluene (Riedel-de Haën GmbH) was used as solvent for sorption and desorption experiments.

The solvent weight fraction corresponding to the glass transition (i.e. the concentration at which the glass transition temperature of the polymer solution is equal to the experiment temperature, 25 °C in this study) depends on the copolymer composition [3,4] and is $\omega_{sg} = 0.15$ for the 84/16 copolymer and $\omega_{sg} = 0.09$ for the 48/52 copolymer. These values were obtained in a previous study devoted to the influence of the glass transition on the vapor/liquid equilibrium [5].

2.2. Sample preparation

The polymer films were spin-cast directly onto the gold electrode of piezoelectric quartz crystals. The film thickness must be large enough to get an accurate determination of solvent weight fraction and small enough to avoid large damping of the resonance (Section 3.2). A 410 nm thick film was prepared for the 84/16 copolymer. In order to investigate the influence of thickness, two films with thicknesses 440 and 1100 nm were prepared for the 48/52 copolymer.

The films were spin-cast from a 5% wt solution in toluene. When investigating the surface of the films with a profilometer (Alpha-Stepper 200 from Tencor Instruments), thickness fluctuations in the range of 5–10% of the sample thickness were found. These thickness variations do not affect our results critically.

3. Experimental

3.1. Experimental setup

A detailed description of the experimental setup has been given elsewhere [1,6]. The polymer film cast onto a quartz crystal resonator is located inside a vacuum chamber that is connected through electronic valves to a solvent reservoir (in which the solvent vapor pressure is equal to the saturated vapor pressure of pure solvent, i.e. $P_{vs0} = 28.45$ Torr at $T = 25$ °C for toluene), to a vacuum pump and to a

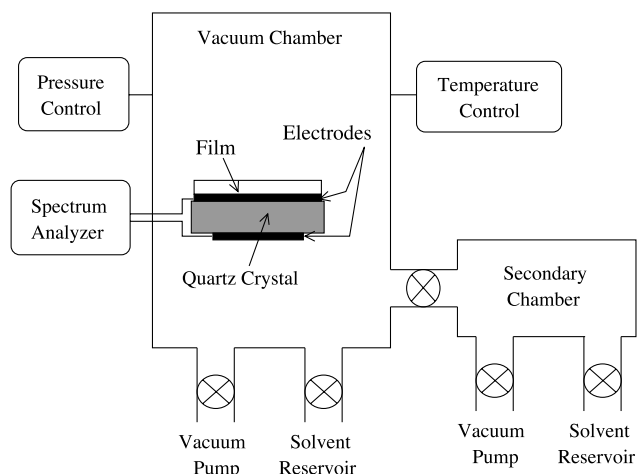


Fig. 1. Experimental setup.

secondary vacuum chamber (Fig. 1). The lowest pressure reached under continuous pumping is 10^{-3} Torr. Since the experiments are undertaken at much larger pressures, this state is called ‘zero pressure’ in the following. Two pressure gauges are used for the ranges $P > 10$ Torr and $P < 10$ Torr. Their accuracy was 0.02 and 0.002 Torr, respectively. The pressure in the chamber is controlled by a PID regulation, allowing to maintain the pressure constant for several hours. Rapid pressure steps are possible by opening the valve connecting the sample compartment to the secondary chamber. Depending on the pressure difference between the two chambers, the step amplitude is between 0.5 and 2 Torr for sorption and between 0.2 and 1 Torr for desorption. This setup allows very reproducible and well-defined differential steps (small activity steps). Note that, as there is no inert gas in the chamber, the pressure in the chamber corresponds to the saturated vapor pressure of the solvent above the polymer film at equilibrium.

Using a thermostat, the chamber temperature is adjusted to $T = 25 \pm 0.15$ °C. This is necessary because of the temperature dependence of quartz crystals resonance frequency.

3.2. Weight determination

Quartz crystal resonators are currently used to determine the weight of thin films [7,8]. When a thin film is cast onto one of the electrodes of a thickness-shear resonator, its acoustical resonance frequencies change due to the weight of the film. For a sufficiently thin film, the relation between weight and frequency shift (for the n th harmonic) is given by the Sauerbrey equation [9]:

$$\delta m = -\frac{Z_q}{2f_1} \left(\frac{\delta f}{f} \right)_n = -\frac{Z_q}{2f_1} \frac{f_n - f_{n,\text{ref}}}{f_{n,\text{ref}}} \quad (1)$$

where δm is the film weight per unit area, f_n the frequency of the n th harmonic, $f_{n,\text{ref}}$ the frequency of the n th harmonic for

the unloaded quartz, f_1 the fundamental frequency, and $Z_q = 8.8 \times 10^6 \text{ kg m}^{-2} \text{ s}^{-1}$ the acoustic impedance of AT-cut quartz. Weight estimated from one harmonic (with n usually 3 or 4) using the Sauerbrey equation is called ‘linear weight’ in the following. However, the Sauerbrey equation is valid only for thin films whose thicknesses are much less than the wavelength of sound $[f_n \sqrt{\rho |J|}]^{-1}$, where ρ is the film density and J its complex shear compliance ($J = J' + J''$). For thicker or softer films, viscoelastic behavior has to be taken into account and the relation between weight and frequency shifts becomes [10,11]:

$$\left(\frac{\delta f}{f} \right)_n = \frac{f_n - f_{n,\text{ref}}}{f_{n,\text{ref}}} = -\frac{2f_1}{Z_q} \left(\delta m + \frac{4\pi^2}{3} \frac{J' \delta m^3}{\rho} f_n^2 \right) \quad (2)$$

By plotting $(\delta f/f)_n$ derived from different harmonics versus the square of the frequency f_n^2 , the film weight per unit area corresponds to the offset of the line. In this work, given the film thicknesses, the weights were calculated using harmonics between $n = 2$ and $n = 8$. The weight estimated with this model is called ‘cubic weight’ in the following.

Data acquisition is achieved with an impedance analyzer (Hewlett-Packard HP4195) which allows to determine the frequency-dependent conductance and susceptance of the quartz resonator in the vicinity of an acoustic resonance [6, 10]. The first method uses the conductance curve $G(f)$ to estimate the frequency shift. Weight determination takes about 5 s per data point when using the ‘linear weight’ and 30 s when using the ‘cubic weight’ with six harmonics. We developed another procedure to perform faster data acquisition as needed to follow sorption kinetics of thin films. This method is based on the analysis of the susceptance spectrum $B(f)$, assuming that a shift in resonance frequency only shifts the spectrum without altering it in any other way [6]. The time for data acquisition is decreased to about 0.2 s.

3.3. Errors

Although the quartz crystal microbalance is known to be a very precise tool as frequencies may be measured with a very good accuracy (monolayer sensitivity), the obtained performances in this study were far from the theoretical ones because of the various phenomena that affect weight determination.

First, resonance frequencies of a quartz depend on temperature [7]. In the vacuum ($P = 10^{-3}$ Torr) and around 25 °C, preliminary measurements on several blank quartz plates were done. An over-estimation of the corresponding sensitivity gives:

$$-10^{-6} \text{ kg m}^{-2} \text{ }^\circ\text{C}^{-1} \leq \left. \frac{\partial \delta m}{\partial T} \right|_P \leq 0 \quad (3)$$

Temperature fluctuations in the chamber are about ± 0.15 °C, so that the weight error is lower than $\approx \pm 1.5 \times 10^{-7} \text{ kg/m}^2$.

Resonance frequencies of a quartz also depend on pressure. This effect has three sources: viscous drag of the gas, pressure dependence of the elastic constants of the quartz itself, and sorption or desorption of physisorbed molecules on the quartz surface [7]. Preliminary experiments on blank quartz plates in toluene vapor showed that the systematic error due to pressure effects increases as pressure increases. This sensitivity can be overestimated with a linear interpolation between the following points:

$$\left\{ \begin{array}{ll} 10^{-7} \text{ (kg m}^{-2} \text{ Torr}^{-1}) & \text{at 0 Torr} \\ 10^{-7} \text{ (kg m}^{-2} \text{ Torr}^{-1}) & \text{at 9 Torr} \\ 4.5 \times 10^{-7} \text{ (kg m}^{-2} \text{ Torr}^{-1}) & \text{at 21 Torr} \\ 2.5 \times 10^{-6} \text{ (kg m}^{-2} \text{ Torr}^{-1}) & \text{at 28 Torr} \end{array} \right. \quad (4)$$

Another uncertainty comes from the limitation of the validity domain of the theoretical models of quartz microbalances. Depending on the thickness and softness of the films, more or less important differences have been observed between ‘linear weight’ and ‘cubic weight’, and between the ‘susceptance method’ and ‘conductance method’. The kinetics in Fig. 5(b) displays a typical example of the uncertainty due to the shift from ‘linear weight’ to ‘cubic weight’ (desorption step, $t^{1/2}/e = 10^8 \text{ s}^{1/2}/m$), that is about $4 \times 10^{-8} \text{ kg/m}^2$.

Given the very small solvent uptakes obtained with the experiments performed in this study, these various systematic errors are significant. They can be bounded but not enough accurately determined to allow corrections, so that a specific estimation method has been used to analyze the experimental data (cf. Section 5). This method uses the error characterization detailed above.

3.4. Experimental procedure

In the glassy domain viscoelastic relaxation involves characteristic times of the same order of magnitude than experiment durations and the film does not reach equilibrium. As a consequence, results depend on the entire film history and the whole procedure must be carefully defined. In most of differential sorption or desorption experiments reported in the literature, pressure steps are performed one after the other, like ‘stairs’. We have chosen another experimental procedure (Fig. 2): before each increasing step, the film is kept at high pressure (about 25 Torr) for about 2 h. The film is then very swollen and in the rubbery state, allowing the whole previous story to be ‘forgotten’. Starting from this well-defined rubbery state, the pressure is lowered to the initial pressure chosen for the sorption step. This initial pressure is maintained a few hours until a ‘quasi-equilibrium’ is reached (i.e. solvent diffusion is achieved and weight change due to relaxation is very small). Then the differential increasing pressure step is performed and the final pressure maintained for about 5–10 h. Afterwards a decreasing step of about the same amplitude is performed.

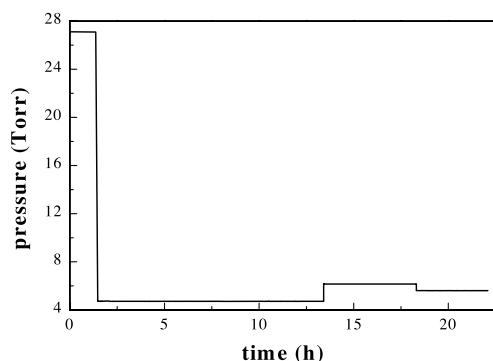


Fig. 2. Experimental procedure—Pressure evolution for the ‘5–6.5 Torr’ sorption step and the ‘6.5–5.9 Torr’ desorption step performed on the 84/16 copolymer.

The solvent weight fractions at the beginning of the different sorption steps are given in Fig. 3 for the 84/16 copolymer. They are compared with the solubility curves obtained when performing slow decreasing or increasing pressure ramps [5]. During the ramps, the pressure changes slowly enough compared to diffusion time to assume a uniform concentration in the film. The influence of the film history is clearly shown for the 84/16 copolymer, whose solvent-induced glass transition occurs around $\omega_{sg} = 0.15$. For a same activity, the amount of solvent in the film during a decreasing pressure ramp is larger than the one during an increasing pressure ramp, showing that the macromolecular matrix is not in equilibrium and that relaxation times are greater than the typical duration of a pressure ramp. The difference between increasing and decreasing ramps is typical of glassy state. The initial solvent weight fractions of the different sorption steps lie between these two curves: indeed, although the initial state is the same than for decreasing ramp (rubbery state), the film is kept a few hours at the initial pressure of the step (in the glassy state) and then has more time to relax than during the decreasing pressure

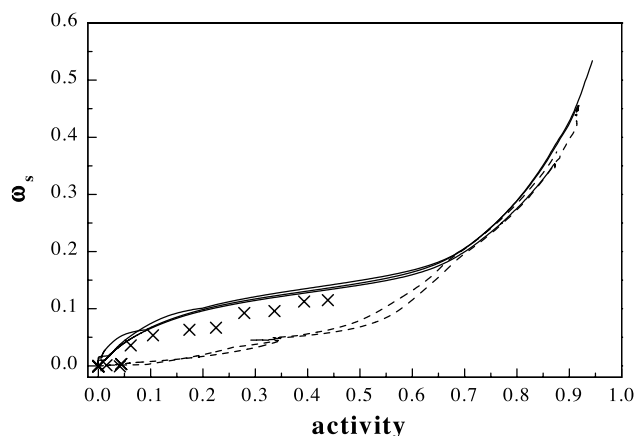


Fig. 3. Sorption (– – –) and desorption (—) solubility curves for the 84/16 copolymer. Comparison with the initial solvent weight fraction of the sorption steps (×).

ramp. This underlines once more the great influence of film history and then the importance of the experimental procedure. The phenomena was found to be less important for the 48/52 copolymer, the solvent-induced glass transition occurring for a smaller solvent content: $\omega_{sg} = 0.09$.

4. Modeling

Many works have concerned solvent diffusion in rubbery and glassy polymer films, and we just recall some main features. Deviation from Fickian kinetics in the glassy state was observed by several authors when performing sorption or desorption experiments, due to the coupling between solvent diffusion through the film and polymer matrix relaxation. Qualitative description of these non-Fickian kinetics highlights various behaviors (sigmoid, pseudo-Fickian, two steps, case II, etc.) depending on the experiment performed (sorption or desorption, differential or large pressure steps), the studied systems and the experimental procedure [12–16].

The Deborah number, $Deb = \tau_r/\tau_d$, is often used to compare the characteristic times of relaxation (τ_r) and diffusion (τ_d) [17]. In the rubbery state, far from the glass transition, relaxation is quasi instantaneous compared to diffusion ($Deb \ll 1$) and classical Fickian kinetics is observed. In the case $Deb \gg 1$, macromolecular configuration evolution has no time to take place during a typical sorption experiment and Fickian kinetics is expected. In the vicinity of the glass transition, Deb is about one and the coupling of the two phenomena leads to complex non-Fickian kinetics.

Several theoretical approaches have been proposed, none of them succeeding in fitting all the non-Fickian kinetics. One of these approaches takes viscoelastic relaxation into account through a constitutive equation, where the viscoelastic behavior is approximated by a Maxwell model [18–21]. A second approach consists in taking the coupling between diffusion and relaxation into account through the boundary condition at the film/vapor interface only (solubility model, [22–24]), which then expresses as:

$$c(z = e, t > 0) = c_d + (c_\infty - c_d) \left[1 - \exp\left(-\frac{t}{\tau_r}\right) \right] \quad (5)$$

where e is the film thickness, c_d the ‘quasi-equilibrium’ concentration (the asymptotic concentration if the only mechanism is diffusion), c_∞ the equilibrium concentration and τ_r the relaxation characteristic time. Unlike the former approach, no new driving term appears in the equation describing solvent transport inside the film that is expressed by the Fick equation (with a constant diffusion coefficient as only differential pressure steps are considered):

$$\frac{\partial c(z, t)}{\partial t} = D_{SP} \frac{\partial^2 c(z, t)}{\partial z^2}, \quad 0 < z < e \quad (6)$$

The only change compared to the classical Fick model

comes from the variation of solubility induced by the time-dependent boundary condition. This simple model is known to allow the description of different types of kinetics [1,22,25,26]. It fits our data very well and has the advantage to involve four parameters only, c_d and D_{SP} for diffusion, c_∞ and τ_r for relaxation.

Practically many macromolecular modes are involved during polymer matrix relaxation and taking the relaxation into account through a first order model is a rough approximation. So we extend the solubility model introducing a relaxation time distribution. Various experiments devoted to the dynamics in glassy systems have been successfully fitted with a stretched exponential, with exponent β varying typically from 0.3 to 0.5 [27,28]. So we also used the following boundary condition that corresponds to an exponent 0.5:

$$c(z = e, t > 0) = c_d + (c_\infty - c_d) \left\{ 1 - \exp\left[-\left(\frac{t}{\tau_r}\right)^{1/2}\right] \right\} \quad (7)$$

with an average time distribution $\langle \tau \rangle = 2\tau_r$.

5. Data fitting method

Given the various uncertainties on the weight measurements, classical least square optimization was not suitable to analyze our data and estimate the parameters of the time dependent solubility model. Indeed, uncertainties on the fitted parameters are well defined in least-square optimization when measurement errors are random. In the case of quartz microbalance technique, the errors due to pressure and temperature effects are systematic. Moreover, when diffusion and relaxation are coupled, the problem is badly conditioned, i.e. close weight kinetics, $\Delta m(t)$, can be obtained with quite different parameters sets. To overcome this difficulty we have used a global optimization method, the set inversion method [29]. The aim is to estimate all the parameter sets ‘ $p = (\tau_d, \tau_r, \Delta m_d, R)$ ’ that give kinetics lying between two a priori bounding curves, where:

$$\Delta m_d = |c_d - c_i|e, \quad \Delta m_\infty = |c_\infty - c_i|e,$$

$$R = \Delta m_d / \Delta m_\infty$$

and c_i the initial concentration.

For each sorption or desorption step, the two bounding curves $\Delta m_{\min}(t)$ and $\Delta m_{\max}(t)$ are calculated from the upper-bound of the different uncertainties described in Section 3.3. These uncertainties are derived from the temperature, pressure and weight measurements. The real kinetics should lie between these two bounding curves. One example is given in Fig. 4. Note that, since the senses of variation of temperature and pressure effects are known, the error amplitudes are not symmetric.

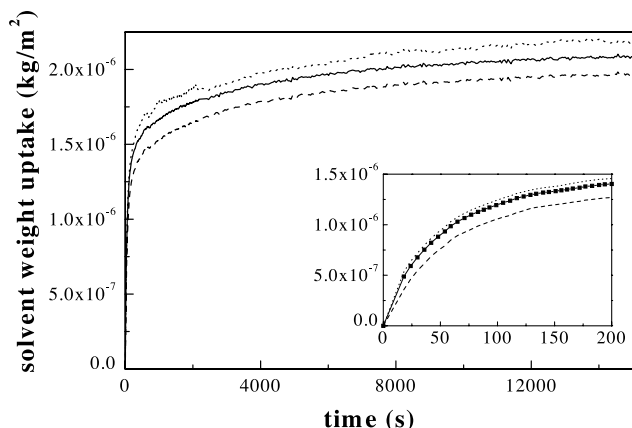


Fig. 4. Evolution of the solvent weight uptake during the '5–6.5 Torr' sorption step for the 410 nm thick film of 84/16 copolymer. The experimental kinetics $\Delta m(t)$ (—) is surrounded by two curves, the lower bound $\Delta m_{\min}(t)$ (---) and the upper bound $\Delta m_{\max}(t)$ (···), taking the various uncertainties described in Section 3.3 into account.

The optimization method is detailed elsewhere [29–32] and we just give the main features of the SIVIA algorithm (Set Inversion Via Interval Analysis). First, a large a priori variation domain is chosen for each parameter, leading to an initial box in the parameters space (dimension = 4):

$$0.1 \text{ s} \leq \tau_d \leq t_{\text{end}}, \quad 0.1 \text{ s} \leq \tau_r \leq 10 \times t_{\text{end}},$$

$$10^{-8} \text{ kg/m}^2 \leq \Delta m_d \leq \Delta m_{\text{end}}, \quad 10^{-3} \leq R \leq 1$$

where t_{end} is the experiment duration (about 2×10^4 s) and Δm_{end} the weight variation obtained at the end of the experiment (about 2×10^{-6} kg/m² for a 500 nm thick film).

An iterative procedure divides this initial box into smaller and smaller boxes that are partitioned in feasible, unfeasible and ambiguous boxes. A box is said feasible (unfeasible) if all its quadruplets ' p ' give kinetics $\Delta m(p, t)$ lying (not lying) between the two bounding curves. Other boxes are said ambiguous. Because the kinetics $\Delta m(p, t)$ is monotonic versus the four parameters (overshoot phenomena are excluded) $\Delta m(p, t)$ is an increasing function of Δm_d and a decreasing function of R , τ_d , τ_r —it is easy to characterize each box by computing the theoretical kinetics associated with the extreme values of the box. After elimination of the unfeasible boxes and selection of the feasible ones, the ambiguous boxes are divided into smaller ones and the procedure is repeated until the ambiguous domain is small enough.

This method has the great advantage to give well-defined uncertainty domain for the four parameters, without favoring any specific solution. Information on the coupling between the estimations of the different parameters is obtained by considering the projections of feasible domains on spaces of dimension 2 or 3. One-dimension projections give the maximum variation domain for each parameter. The method is, however, computer time consuming (a few

hours on a Pentium III 500 MHz computer for the analysis of one weight kinetics).

6. Results

6.1. Qualitative analysis of the sorption/desorption kinetics

Several differential sorption and desorption pressure steps were performed in the glassy state between 0 and 12.3 Torr for the 84/16 copolymer, and between 0 and 6 Torr for the 48/52 copolymer. Examples of kinetics for various pressure steps are given in Fig. 5. The abscissa is $t^{1/2}/e$. The ordinate is $(\omega_s - \omega_{si})/\Delta a$, where ω_s is the solvent weight fraction and ω_{si} its initial value at the beginning of the step. Δa is the activity change during the step ($\Delta a = \Delta P/P_{vs0}$). This coordinate allows the comparison of steps having slightly different pressure amplitudes, and the comparison of sorption and desorption steps. In this

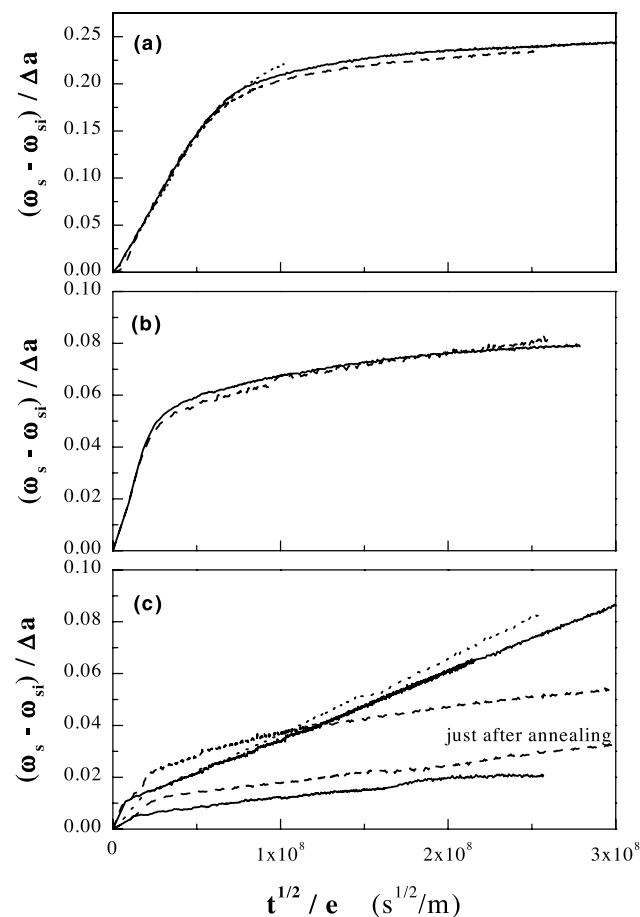


Fig. 5. Experimental kinetics obtained for various pressure steps with the two copolymers. (a) With the 48/52 copolymer, for sorption step '0.8–1.5 Torr' with the 410 nm thick film (—) and for desorption step '1.5–0.8 Torr' with the 410 nm thick film (---) and the 1100 nm thick film (···). (b) With the 84/16 copolymer, for sorption step '5–6.5 Torr' (—) and desorption step '6.5–5.9 Torr' (---). (c) Sorption (—) and desorption (---) kinetics obtained for various pressure steps from and towards 0 Torr ('zero pressure') with the 84/16 copolymer.

representation, Fickian kinetics corresponds to a linear increase at short times and to the saturation towards an asymptotic value at large times.

As expected for the experiments performed at a low pressure corresponding to the glassy domain (Fig. 3), the kinetics curves are clearly non-Fickian. Many of them are close to the so-called pseudo-Fickian kinetics, which exhibits a linear part at short times followed by a slow increase of $(\omega_s - \omega_{si})/\Delta a$. However, contrary to some authors, no S-shape or two-stages curves were observed whatever the pressure. Finally let us notice that:

- As expected the kinetics observed for the two films of 48/52 copolymer having different thicknesses (440 and 1100 nm) are similar at short times in the $t^{1/2}/e$ graph (Fig. 5(a)).
- In the range of accuracy of our measurements, sorption and desorption kinetics are similar at least at short times when diffusion is dominating (Fig. 5(a) and (b)). This also confirms the assumption of differential steps. The difference that appears at the end of the experimental duration may come from either external effects (temperature drift for example) or from intrinsic phenomena such as very long relaxation times. Experimental data are actually not sufficient to go further in the interpretation of long-range behaviors.
- All the kinetics show a good reproducibility, except for the steps from and towards 0 Torr (Fig. 5(c)). These odd behaviors at 0 Torr are still not understood despite various explanations can be suggested: the assumption of linearity (differential steps involving a constant diffusion coefficient) may be erroneous, since the diffusion coefficient could decrease very strongly near 0 Torr, i.e. when solvent concentration goes to zero. Some authors put forward the development of longitudinal stresses in the viscoelastic film [13]. Given the misunderstood behavior of the sorption or desorption steps from or towards 0 Torr, we do not take these data into account in the study of the diffusion coefficient.

6.2. Quantitative analysis

For each sorption and desorption step, the SIVIA algorithm was used to estimate the four parameters of the time dependent solubility model: τ_d , τ_r , Δm_d , R . To allow comparison, the results are given using the following variables: the diffusion is characterized by the mutual diffusion coefficient D_{SP} and by the change in solvent weight fraction induced by the diffusion for an activity step equal to one, $\Delta\omega_d/\Delta a$. The relaxation is characterized by the relaxation time τ_r and by the change in solvent weight fraction induced by the relaxation for an activity step equal to one,

$$\frac{\Delta\omega_r}{\Delta a} \simeq \left(\frac{1}{R} - 1\right) \frac{\Delta\omega_d}{\Delta a}.$$

It is to note that there is some ambiguity to estimate the exact

value of the polymer weight in our experiments (and then to estimate the solvent weight fraction), since the weight of the film at 0 Torr was shown to increase all along the experiments. This increase may be due to some trapped solvent or/and to some drift of the microbalance. This point has been thoroughly described in the previous study performed on the same copolymers [5]. We have used the same method of estimation of the polymer weight in this paper and checked that this choice does not change the results significantly.

6.2.1. Set inversion projections

Examples of 2D projections derived from the set inversion analysis are given in Fig. 6 for a sorption step (5–6.5 Torr) performed on the 84/16 copolymer (Fig. 5(b)).

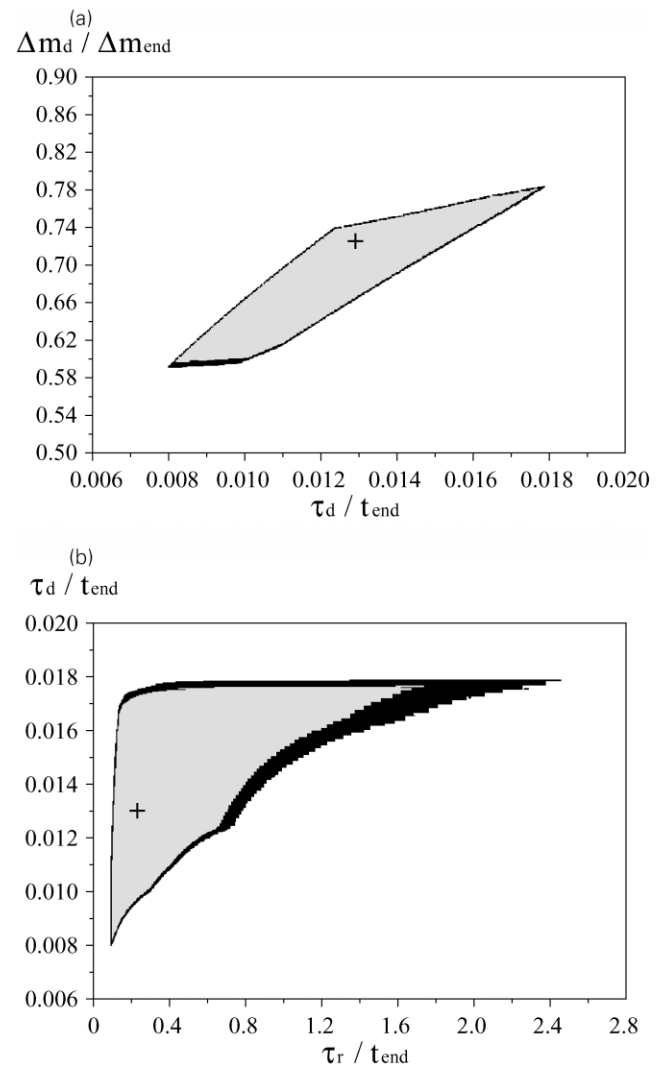


Fig. 6. Zoom around the feasible domain (gray area) and ambiguous domain (black area) of the 2D projections derived from the set inversion analysis for the '5–6.5 Torr' sorption step experiment performed on the 84/16 copolymer, for the two parameters (a) $\Delta m_d / \Delta m_{end}$ and τ_d / t_{end} , (b) τ_d / t_{end} and τ_r / t_{end} . The experimental horizon and total solvent weight uptake used to define the initial box are $t_{end} = 15,423$ s and $\Delta m_{end} = 2.08 \times 10^{-6}$ kg/m². The symbol '+' corresponds to the least-square solution.

The gray area corresponds to the feasible domain, the white area to the no-feasible domain and the black frontier to the ambiguous one. The horizon (experimental duration) and total solvent weight uptake used to define the initial box are $t_{\text{end}} = 15,423$ s and $\Delta m_{\text{end}} = 2.08 \times 10^{-6}$ kg/m². For clarity, the Fig. 6(a) and (b) correspond to a zoom around the feasible domain.

In this example, the variation domain is small for τ_d , with a factor less than 2.5 between the two admissible extreme values of τ_d ($120 \text{ s} \leq \tau_d \leq 275 \text{ s}$, i.e. $0.6 \times 10^{-15} \leq D_{\text{SP}} \leq 1.4 \times 10^{-15} \text{ m}^2/\text{s}$). The weight uptake due to diffusion is about 60–80% of Δm_{end} . There is a strong correlation between the two parameters characterizing the diffusion (Fig. 6(a)), large values of τ_d being associated with large values of Δm_d , as expected if considering classical diffusion behavior. Practically, the experimental data contain enough information on diffusion to allow an accurate estimation of the mutual diffusion coefficient.

On the contrary, as can be seen in Fig. 6(b), the feasible domain for τ_r is large (1380–36,700 s). For small values of τ_r , diffusion and relaxation are strongly coupled, which makes the estimation of both parameters difficult and leads to the less accurate estimation of τ_d . For comparison, the solution corresponding to the classical least square solution is also marked on the figure ($\tau_d = 1905$ s, $\tau_r = 2990$ s, $\Delta m_d = 1.51 \times 10^{-6}$ kg/m², $R = 0.73$).

This analysis of the different 2D projections was performed for the various experiments and leads to the following conclusions:

- The significant area of the feasible domains highlight the ill-conditioned character of this estimation problem, due partly to the limited horizon and to the large amplitude of experimental uncertainties.
- In most of the experiments, bounded domains were obtained for the two parameters characterizing diffusion (i.e. the feasible domain is strictly included in the initial box) while results on relaxation were less satisfactory, the two parameters characterizing the relaxation being often no upper-bounded. This means that information brought by the data on relaxation phenomena is too poor to get significative estimation.

Let us emphasize that the classical least-square minimization would have given one quadruplet only for each experiment, with a surely questionable physical meaning, especially for relaxation.

In the following only one dimensional projections are considered and the variation domain of a given parameter gives all the feasible and ambiguous values of this parameter. Let us now discuss the results obtained for various solvent contents in the film.

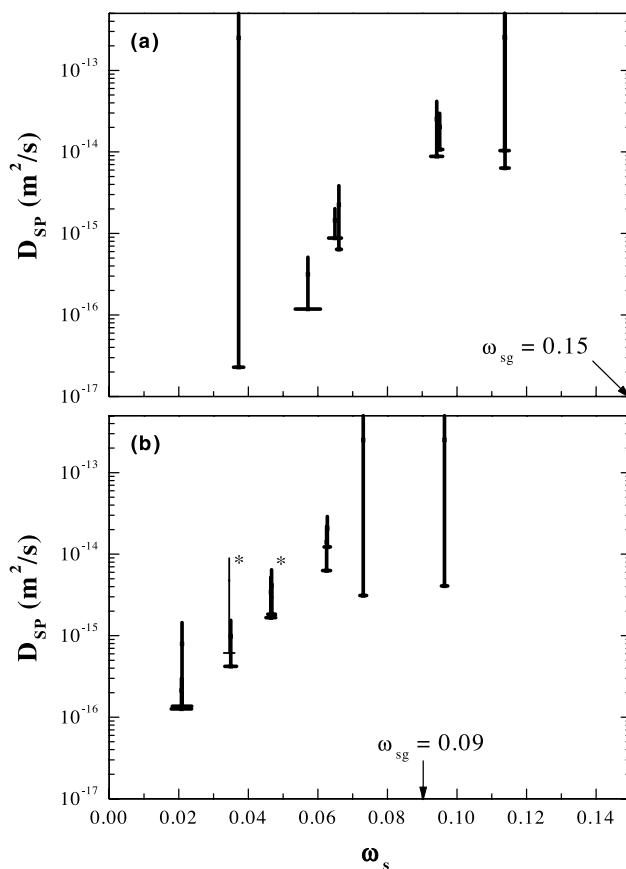


Fig. 7. Mutual diffusion coefficient D_{SP} (semi-logarithmic scale) versus solvent weight fraction ω_s , for (a) the 84/16 copolymer and (b) the 48/52 copolymer. The experiments performed on the 1100 nm thick film of the 48/52 copolymer are marked with *.

6.2.2. Mutual diffusion coefficient

The variations of the mutual diffusion coefficient with the solvent weight fraction are reported for the two copolymers in Fig. 7(a) and (b). The results are represented in the following way. The horizontal bar corresponds to the solvent weight fraction covered during the step; as can be seen, this variation is very small (often smaller than 0.01), as required by the assumption of differential sorption or desorption. The vertical bar corresponds to the feasible and ambiguous domains issued from the set inversion method. When no upper bound is obtained, the vertical bar is drawn up to the graph frame. Most of the steps were performed in the glassy domain, the solvent-induced glass transition occurring for $\omega_{\text{sg}} = 0.15$ and 0.09 for the 84/16 and 48/52 copolymers, respectively.

The quantitative analysis confirms the results observed on the weight kinetics: the estimated diffusion coefficients obtained from sorption and desorption experiments are close (validating the assumption of differential steps), as well as the values obtained from the two 48/52 copolymer films of different thickness.

For the two copolymers, the mutual diffusion coefficient D_{SP} decreases strongly as the solvent concentration

decreases: about two orders of magnitude for a 0.05 change in ω_s (Fig. 7). Contradictory results have been reported in the literature. Indeed, results similar to ours were obtained by Boom and Sanoupolou on the system PMMA/methylacetate [26]. On the contrary, Billovits and Durning observed a large difference in the variations in the rubbery and glassy domains, obtaining a nearly constant diffusion coefficient in the glassy domain for the system PS/ethylbenzene [12]. Sun also obtains a plateau in the glassy domain for the system PHEMA/water [33]. This plateau was interpreted as the consequence of large slowing down in free volume decreasing due to the glass transition, and Duda et al. had modified the free volume model that describes the variation of diffusion coefficients with concentration to take this effect into account [34].

These qualitatively different behaviors show that the influence of glass transition on the diffusion coefficient is a complex problem that is still not deeply understood. Among other points, it should be interesting to go deeper in the analysis of the respective influences of the system itself (physico-chemistry of the polymer/solvent solution), the experimental procedure (influence of the solvent activity history undergone by the film) and the distance to the glass transition. An extension of this study to a larger family of PMMA/*Pn*BMA copolymers has been undertaken and will give additional results on these points.

6.2.3. Solvent weight uptake induced by diffusion and relaxation

A slight decrease of the normalized solvent weight uptake due to diffusion ($\Delta\omega_d/\Delta a$) seems to appear as the solvent concentration increases, however, the uncertainties are too large to give a firm conclusion. It is interesting to compare these values of solvent weight uptake only due to diffusion to the one deduced from the solubility curves obtained when performing slow pressure ramps. Let us recall that during ramps, the pressure evolves slowly so that the concentration can be assumed uniform in the film, while relaxation is not completely achieved. The derivative of the solubility curve was shown to be much higher than the values estimated from the sorption/desorption kinetics, highlighting that the contribution of relaxation is important during ramps. A more precise comparison would need to introduce the estimated values for $\Delta\omega_r/\Delta a$. However, the present study being mainly devoted to diffusion, the measurement horizon of each sorption or desorption experiment was not long enough to get an accurate estimation of $\Delta\omega_r$ (often not upper bounded).

6.2.4. Relaxation time

The relaxation time τ_r of the solubility model was also estimated (Fig. 8(a) and (b)). Due to the limited measurement horizons, it was not always possible to get the upper bound of the variation domain for this parameter. However,

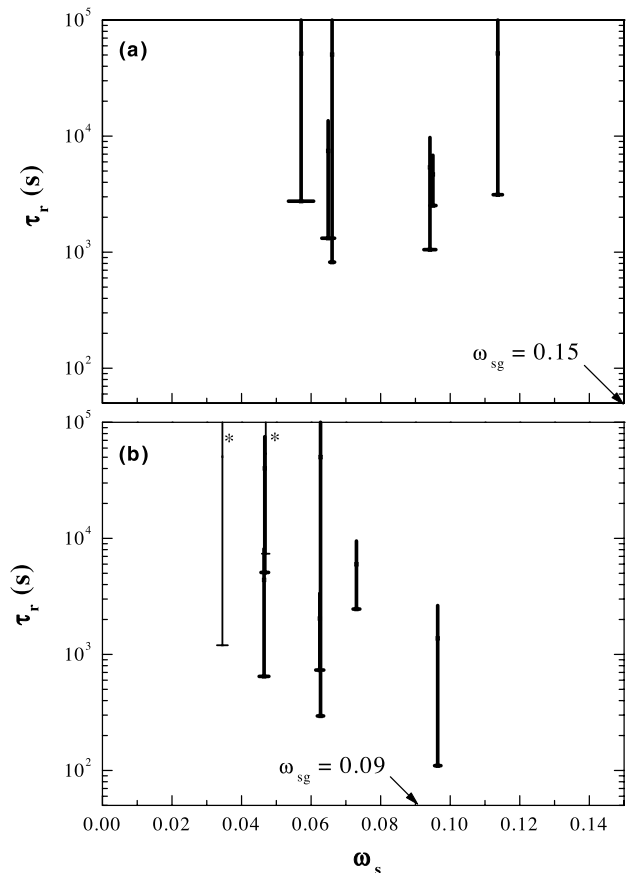


Fig. 8. Relaxation time τ_r versus solvent weight fraction ω_s , for (a) the 84/16 copolymer and (b) the 48/52 copolymer. The experiments performed on the 1100 nm thick film of the 48/52 copolymer are marked with *.

for all the experiments a relaxation term was needed to fit the data, that shows once more the non-Fickian character of the kinetics. The lower bound of τ_r is most often greater than the upper bound of the characteristic diffusion time τ_d , which confirms that diffusion is predominant at short times while relaxation dominates at the end of the horizon. When they are bounded, the obtained values are rather smaller than values reported in the literature for other system: about 10^5 s for PHEMA/water [35] or PMMA/methyl acetate [26], 5×10^2 – 5×10^3 s for PS/ethylbenzene [12,36].

6.3. Comparison with a relaxation time distribution model

As previously said, the validity of a description involving only one time of relaxation is not obvious, since polymer matrix relaxation involves many relaxation modes. It is then important to check the robustness of the results, especially on the diffusion coefficient, when changing the relaxation description in the solubility model. The analysis with the set inversion method was renewed introducing the stretched exponential time distribution described in Section 4. For almost all the experiments, it was not possible to determine the upper bound of the average time $\langle\tau\rangle$, that means that a

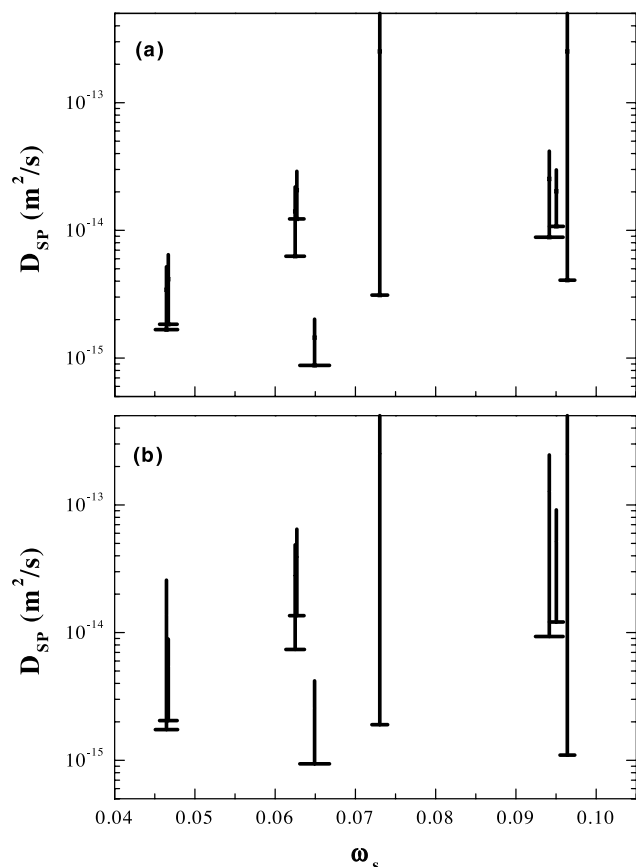


Fig. 9. Mutual diffusion coefficient D_{SP} (semi-logarithmic scale) versus solvent weight fraction ω_s for the 2 copolymers, (a) derived from the one relaxation time model and (b) the relaxation time distribution model.

meaningful study of relaxation should need much larger horizons and that much care must be taken in the interpretation of the characteristic time estimated with a description using only one relaxation time. On the contrary, results concerning diffusion were not modified by the introduction of a relaxation time distribution, as can be seen on Fig. 9 (the uncertainty domain of D_{SP} being slightly increased for some experiments). In the domain of solvent weight fraction investigated here, the predominance of diffusion at short times is strong enough to allow a robust estimation of the diffusion coefficient.

7. Conclusion

A detailed analysis of differential sorption and desorption kinetics have been performed for two copolymers P(MMA/*n*BMA) in the glassy domain. The gravimetric experiments were performed with a quartz microbalance on thin films (about 400 and 1100 nm thick). For each experiment, the experimental procedure consists in a preliminary stay at high pressure (in the rubbery domain) to forget the film history. The pressure is then lowered to the initial pressure of the sorption step and maintained constant

a few hours. Then the measurement is performed by applying two successive differential steps (a sorption one and a desorption one). Special care was given to the estimation of all the experimental uncertainties due to temperature and pressure effects, as well as to frequencies data interpretation. The coupling between diffusion and relaxation was taken into account through the time dependent solubility model. This model depends on four parameters, describing characteristic times and weight uptakes due to diffusion on one hand and relaxation on the other hand. Given the experimental uncertainties and the coupling between the two phenomena, a global estimation method was developed to get a reliable determination of the four parameters. This global optimization method gives all the parameters sets consistent with the experimental accuracy. As a consequence, it highlights the information really exploitable in the experimental results for a meaningful physical interpretation.

Contrary to several authors, we have not observed a large slowing down in the variations of the diffusion coefficient in the glassy state: D_{SP} strongly decreases for the two copolymers, of about two orders of magnitude for a 0.05 decrease in ω_s . Concerning the relaxation, two descriptions have been compared: the first one uses one relaxation time only while the second one involves a relaxation time distribution, closer to the physical description of glass transition. As shown by the SIVIA results and given the limited horizons of our experiments, it was not possible to get accurate conclusions on the most appropriate model nor on the evolution of relaxation times with concentration, but the estimation of the diffusion coefficient was not significantly affected by the choice of the relaxation description. A detailed presentation on the application of a set inversion method to analyze the data for two copolymers is given here. In a next study, we will present the results obtained by this method for a family of copolymers of various compositions, in order to investigate systematically the evolution of diffusion coefficient with both solvent concentration and copolymer composition.

Acknowledgements

This work was supported by PEFE (Pechiney Emballage Flexible Europe) and by a PROCOPE project (French–German Cooperation Program, no. 134). The numerical calculations have been performed on the computers of the ‘Centre National de Calcul’ of CNRS (IDRIS), and of the ‘Centre de Calcul Recherche’ of the University Pierre et Marie Curie (Paris).

References

- [1] Saby-Dubreuil A.-C. Séchage de films polymères : Etude du couplage entre la diffusion et la transition vitreuse—Application à des

- copolymères PMMA/PnBMA, PhD Thesis, de l'université Paris VI, 2001.
- [2] Brar A, Kapur G. *Polym J* 1988;20(9):811–7.
- [3] Chow T. *Macromolecules* 1980;13:362–4.
- [4] Kelley F, Bueche F. *J Polym Sci* 1961;L:549–56.
- [5] Saby-Dubreuil A-C, Guerrier B, Allain C, Johannsmann D. *Polymer* 2001;42:1383–91.
- [6] Bouchard C, Guerrier B, Allain C, Laschitsch A, Saby A-C, Johannsmann D. *J Appl Polym Sci* 1998;69:2235–46.
- [7] Lu C, Czanderna A. *Applications of piezoelectric quartz crystal microbalances*. Amsterdam: Elsevier; 1984.
- [8] Stockbridge C. *Vacuum microbalance techniques*. New York: Plenum; 1966.
- [9] Sauerbrey G. *Arch Elektrotech Ubertragung* 1964;18:617.
- [10] Johannsmann D, Mathauer K, Wegner G, Knoll W. *Phys Rev B* 1992; 46:7808–15.
- [11] Domack A, Johannsmann D. *J Appl Phys* 1996;80:2599.
- [12] Billovits G, Durning C. *Macromolecules* 1994;27:7630–44.
- [13] Sanopoulou M, Roussis P, Petropoulos J. *J Polym Sci* 1995;33: 993–1005.
- [14] Sanopoulou M, Roussis P, Petropoulos J. *J Polym Sci* 1995;33: 2125–36.
- [15] Rossi G, Pincus P, De Gennes P. *Europhys Lett* 1995;32(5):391–6.
- [16] Aminabhavi T, Phayde H. *J Appl Polym Sci* 1995;57:1419–28.
- [17] Vrentas J, Jarzebski C, Duda J. *AIChE J* 1977;21(5):895–901.
- [18] Thomas N, Windle A. *Polymer* 1982;23:529–42.
- [19] Durning C. *J Polym Sci* 1985;23:1831–55.
- [20] Edwards D, Cohen D. *AIChE J* 1995;41:2345–55.
- [21] Witelski T. *J Polym Sci B* 1996;34:141–50.
- [22] Long F, Richman D. *J Am Chem Soc* 1960;82:513–9.
- [23] Frisch HL. *J Chem Phys* 1964;41(12):3679–83.
- [24] Berens A, Hopfenberg H. *Polymer* 1978;19:489–96.
- [25] Sanopoulou M, Petropoulos J. *Polymer* 1997;23:5761–8.
- [26] Boom J, Sanopoulou M. *Polymer* 2000;41:8641–8.
- [27] Debolt MA, Eastel AJ, Macedo PB, Moynihan CT. *J. Am. Ceram Soc.* 1976;59:16.
- [28] Brunacci A, Cowie J, Ferguson R, McEwen I. *Polymer* 1997;4: 865–70.
- [29] Walter E, Pronzato L. *Identification of parametric models from experimental data*. London: Springer; 1997.
- [30] Moore R. *Math Comput Simul* 1992;34:113–9.
- [31] Jaulin L, Walter E. *Math Comput Simul* 1993;35:123–37.
- [32] Jaulin L, Walter E. *Automatica* 1993;29(4):1053–64.
- [33] Sun Y, Lee H. *Polymer* 1996;37(17):3915–9.
- [34] Duda J, Romdhane I, Danner R. *J Non-Cryst Solids* 1994;172: 715.
- [35] Sun Y. *Polymer* 1996;37(17):3921–8.
- [36] Huang S, Durning C. *J Polym Sci B* 1997;35:2103–19.